ACS Sustainable Chemistry & Engineering

Research Article

pubs.acs.org/journal/ascecg

First-Row Transition Metal-Containing Ionic Liquids as Highly Active Catalysts for the Glycolysis of Poly(ethylene terephthalate) (PET)

Qian Wang,[†,‡] Yanrong Geng,[†] Xingmei Lu,*[,†] and Suojiang Zhang*[,†]

[†]Beijing Key Laboratory of Ionic Liquids Clean Process, Key Laboratory of Green Process and Engineering, Institute of Process Engineering, Chinese Academy of Sciences, Beijing 100190, P.R. China

[‡]College of Chemistry, Chemical Engineering and Materials Science, Shandong Normal University, Jinan, Shandong 250014, P.R. China

Supporting Information

ABSTRACT: First-row transition metal-containing ionic liquids (ILs) were synthesized and used to catalyze the degradation of poly(ethylene terephthalate) (PET) in ethylene glycol (EG). One important feature of these IL catalysts is that they have good thermal stability, and most of them, especially $[bmim]_2[CoCl_4]$ (bmim = 1-butyl-3-methylimidazolium) and $[bmim]_2[ZnCl_4]$, exhibit higher catalytic activity, compared with traditional catalysts, conventional IL catalysts, and some functional ILs. For example, utilizing $[bmim]_2[CoCl_4]$ as catalyst, the conversion of PET, selectivity of bis(hydroxyethyl) terephthalate (BHET), and mass fraction of BHET in products reach up to 100%, 81.1%, and 95.7%, respectively, under atmospheric pressure at 175 °C for only 1.5 h. Another important feature is that BHET can be easily separated from these IL catalysts and has high purity. Moreover, recycling results show that $[bmim]_2[CoCl_4]$ worked efficiently after being used six times. These all show that $[bmim]_2[CoCl_4]$ is an excellent IL catalyst for the glycolysis of PET. Finally, based on in situ IR spectra and experimental results, the possible mechanism of degradation with synthesized IL is proposed.

KEYWORDS: *Transition metal-containing ionic liquids, Catalyze, Glycolysis, Poly(ethylene terephthalate), Mechanism*

INTRODUCTION

Poly(ethylene terephthalate) (PET) is one of the multifunctional plastics that is widely used as mineral water bottles, soda bottles, food packaging, synthetic fibers, and insulation materials.[1−5] The annual world global consumption of PET packaging was almost 15.5 million tons in 2009, while it is expected to reach 19.1 million tons by 2017, a 5.2% increase per annum.[6] With such a large consumption, the effective recycling of PET wastes has become an important issue in the polyester industry and is one of the most important ways of changing "white pollution" into "green resources". At present, the recycling of PET wastes mainly depends on chemical and physical methods. The quality of the product obtained by the physical method is poor, while the corresponding monomers or raw chemicals could be successfully obtained in chemical recycling and reused for the production of plastic or other advanced materials with good quality.[7,8] So chemical recycling is the most attractive method and has been widely studied. Several chemical degradation methods such as methanolysis, hydrolysis, and glycolysis have been reported. Glycolysis is important because the method has the following advantages: (1) Reaction conditions are milder. (2) The solvent is less volatile. (3) The main product bis(hydroxyethyl) terephthalate (BHET) can be used to make dimethyl terephthalate-based or terephthalic acid-based PET production units, textile softener, and unsaturated polyester resins.[9] It was reported that metal acetates, such as zinc acetate, manganese acetate, cobalt acetate, and lead acetate[10−12] can catalyze the degradation of PET wastes, but higher temperature and pressure are usually needed. Also, the product is difficult to separate from the catalysts. So the development of new catalysts that can effectively degrade PET wastes into BHET under milder conditions is important.

Ionic liquids (ILs) are endowed with environmentally friendly solvents and catalysts and have been widely studied due to their unique properties, such as nonflammability, negligible volatility, high conductivity, and a wide electrochemical window.[13−20] Among these, metal-containing ILs, as a promising subclass of charged liquids, have a more promising application potential and have been one of the current research focuses because they combine the properties of ILs with catalytic, photophysical/optical, or magnetic properties of the incorporated metal salts.[21−27] ILs that contain aluminum, palladium, gold, ruthenium, and platinum (but also iron, zinc, copper, or nickel) have been successfully used in catalysis.[28,29] It has been reported that ILs could be used in the degradation of PET, and metal-containing ILs showed good catalytic activity. Troev et al. found that depolymerization of poly(ethylene terephthalate) fiber proceeds faster in the presence of titanium(IV) phosphate compared with traditionally used compounds like $ZnAc_2$.[11] Our previous work found that

Received: November 25, 2014
Revised: January 5, 2015
Published: January 14, 2015

DOI: 10.1021/sc5007522
ACS Sustainable Chem. Eng. 2015, 3, 340−348

conventional ILs,[9] Fe-containing magnetic IL,[22] and metallic acetate ILs[25] all can be used to catalyze the degradation of PET. Although both PET convention and BHET selectivity are not high enough, the catalytic activity is constantly improved, which explains that the catalytic efficiency can be enhanced by appropriate functional design for ILs, especially the metal functionalization of the ions of ILs.

In this study, first-row transition metal-containing ILs were synthesized and characterized by TGA and element analysis (Supporting Information), and these IL catalysts were used to catalyze the glycolysis of PET. Higher conversion of PET, selectivity of BHET, and mass fraction of BHET in products can be obtained using most of this type of ILs under moderate reaction conditions. The influences of experimental parameters on the degradation of PET were investigated when $[bmim]_2[CoCl_4]$ was used as the catalyst. The recycling use of the catalyst and residual solvent were carried out. Moreover, the possible mechanism of the degradation process with the new catalysts was proposed based on in situ IR and experimental results.

MATERIALS AND METHODS

Experimental Materials. PET pellets (2.0 mm × 2.5 mm × 2.7 mm, ∼30 mesh) were supplied by Jindong Commercial Co., Ltd., Jiangsu Province, China. Their average molecular weight was measured in a 60:40 (w/w) phenol/1,1,2,2-tetrachloroethane solution at 25 °C and was found to be 2.63×10^4 g mol^{-1}. 1-Butyl-3-methylimidazolium chloride ([bmim]Cl) was purchased from Henan Lihua Pharmaceutical Co., Ltd., China. The other reagents for synthesizing ILs and degrading PET, such as manganese dichloride ($MnCl_2$), anhydrous ferric trichloride ($FeCl_3$), cobalt dichloride ($CoCl_2$), nickel chloride ($NiCl_2$), copper chloride ($CuCl_2$), zinc chloride ($ZnCl_2$), chromic chloride ($CrCl_3$), dichloromethane, EG, phenol, and 1,1,2,2-tetrachloroethane (99% purity), were obtained from Sinopharm Chemical Reagent Beijing Co., Ltd., China. The materials were used without further treatment. ILs were synthesized according to the synthesis methods of the other metal-containing ILs.[22−26]

Synthesis of ILs. A series of first-row transition metal-containing ILs were synthesized by mixing the crystal powder of [bmim]Cl with $MnCl_2$, $CoCl_2$, $NiCl_2$, $CuCl_2$, or $ZnCl_2$ with a molar ratio of [bmim]Cl to metal chloride of 2:1 at 50−80 °C for 5−8 h ([bmim]Cl with $FeCl_3$ and $CrCl_3$ at 1:1 at 50 °C for 3 h) until the clear, transparent, homogeneous target liquids appear. The obtained ILs were extracted with small portions of dichloromethane and then water at least three times. The residual dichloromethane and water in ILs were evaporated by a vacuum rotary evaporator at 50 °C, and finally, the resulting clear colorful ILs were dried in a vacuum oven at 60 °C for 24 h. These ILs have been characterized by TGA and element analysis to confirm the structures of the ILs, and one of them is shown in Figure S1 and Table S1 of the Supporting Information. TGA curve of [bmim]Cl was compared with that of Co-containing IL, which indicated that Co-containing IL had a higher thermal stability than [bmim]Cl, and the IL is not the physical mixture of [bmim]Cl and $CoCl_2$. Table S1 shows that the measured values of every elements in the Co-containing IL are consistent with the theoretical values of $[bmim]_2[CoCl_4]$, which indicates that the synthesized IL is $[bmim]_2[CoCl_4]$. The characterations and analysis of the other ILs are similar to that of $[bmim]_2[CoCl_4]$. The results show that the obtained ILs are $[bmim][CrCl_4]$, $[bmim][MnCl_3]$, $[bmim][FeCl_4]$, $[bmim]_2[NiCl_4]$, $[bmim]_2[CuCl_4]$, and $[bmim]_2[ZnCl_4]$.

General Procedure for Catalytic Degradation of PET. In each experiment, the PET pellets, ILs, and EG with a certain weight were charged into a 50 mL round-bottomed three-necked flask equipped with a thermometer and a reflux condenser. The degradation reactions were carried out under atmospheric pressure at reaction temperatures ranging from 130 to 190 °C for reaction times of 0.5−4 h. The flask was immersed in an oil bath at a specific temperature for the required time. When each reaction finished, the reaction mixture was cooled to room temperature. Then an excess amount of distilled water was added to separate the undepolymerized PET pellets from the products. The undepolymerized PET was dried at 70 °C to constant weight and weighted to calculate the conversion of PET, which is defined by eq 1

$$\text{Conversion of PET} = \frac{W_0 - W_1}{W_0} \times 100\% \quad (1)$$

where W_0 represents the initial weight of PET, and W_1 represents the weight of undepolymerized PET. Meanwhile, the degradation products were separated according to the separation method that is the same or similar system in the literatures.[5,9,22,23] The degradation products were vigorously agitated after about 900 mL of cold distilled water was added and then filtered (the distilled water would dissolve the remaining EG, catalyst, and monomer). The collected filtrate in this step was concentrated to about 70 mL by vacuum rotary evaporator at about 50 °C. The concentrated filtrate was stored in a refrigerator at 0 °C for 12 h. White needle-like crystals were formed in the filtrate and then filtered and dried. This was the main product, and characterization shows that it is a BHET monomer. The insoluble fraction in water was dimers and oligomers. The selectivity of BHET and mass fraction of BHET in products are calculated, respectively, using eqs 2 and 3

$$\text{Selectivity of BHET} = \frac{\text{moles of BHET}}{\text{moles of depolymerized PET units}} \times 100\% \quad (2)$$

$$\text{Mass fraction of BHET in products} = \frac{\text{weight of BHET}}{\text{weight of all products}} \times 100\% \quad (3)$$

Analytical Methods. Elementary analysis results of ILs and the main product were performed by a Vario EL cube (Elementar, Germany). The main product was analyzed by NMR (ECA-600, JEOL, Japan) in a d_6-DMSO solution. The GC-MS spectrum was collected using a 6890N Network GC system and a 5975B intert MSD (Agilent, U.S.A) with an Agilent 19091s-433 column under the conditions of an oven temperature of 230 °C, injection temperature of 230 °C, and solvent acetonitrile. Mass spectra were performed on a microTOF instrument (Bruker, Germany) with electrospray ionization (ESI). The UPLC spectrum was measured using a ACQUITY UPLC with TUV detector and BET C_{18} column (Waters, U.S.A.). FT-IR spectra were obtained using a Nicolet 380 spectrometer (Thermo Fisher Scientific, U.S.A.). XRD spectra of the main product and PET material were tested by a D_8 Focus (Bruker, Germany), and SEM images were examined by A XL30S-FEG scanning electron microscopy (Philips, Holand) operated at 40 kV and 10 mA with nickel filtered Cu Kα radiation (λ = 1.54060 Å). The DSC scan of the main product was obtained using DSC1 (Mettler-Toledo, Switzerland) by heating from room temperature to 200 °C at a rate of 10 °C/min in an atmosphere of nitrogen. DTG-60H (SHIMADZU, Japan) was used to measure the weight loss of the ILs, product, and PET material in a nitrogen atmosphere during a temperature range from room temperature to 700 °C, also at a heating rate of 10 °C/min.

RESULTS AND DISCUSSION

Thermal Stability Analysis of ILs. The decomposition temperatures of all the synthesized ILs have been summarized in Table 1. These metal-containing ILs showed outstanding thermal stability as inferred from thermogravimetric results. The decomposition temperature of metal-free IL [bmim]Cl has also been tested for comparison purposes to evaluate how the connection of complexation anions affects the thermal stability. As shown in the same table, the introduction of complexation anions into ILs significantly enhanced their thermal stability.[27]

Qualitative Analysis of the Main Product. The main product obtained in the degradation of PET in EG catalyzed by

DOI: 10.1021/sc5007522
ACS Sustainable Chem. Eng. 2015, 3, 340−348

Table 1. Decomposition Temperature of the Synthesized ILs

ILs	decomposition temperature (°C)
[bmim][$CrCl_4$]	333.28
[bmim][$MnCl_3$]	310.81
[bmim][$FeCl_4$]	361.26
[bmim]$_2$[$CoCl_4$]	270.55
[bmim]$_2$[$NiCl_4$]	331.89
[bmim]$_2$[$CuCl_4$]	269.92
[bmim]$_2$[$ZnCl_4$]	327.77
[bmim]Cl	244.49

[bmim]$_2$[$CoCl_4$] was characterized by GC-MS, NMR, ESI-MS, UPLC, and element analysis. The GC-MS spectrum (Figure 1)

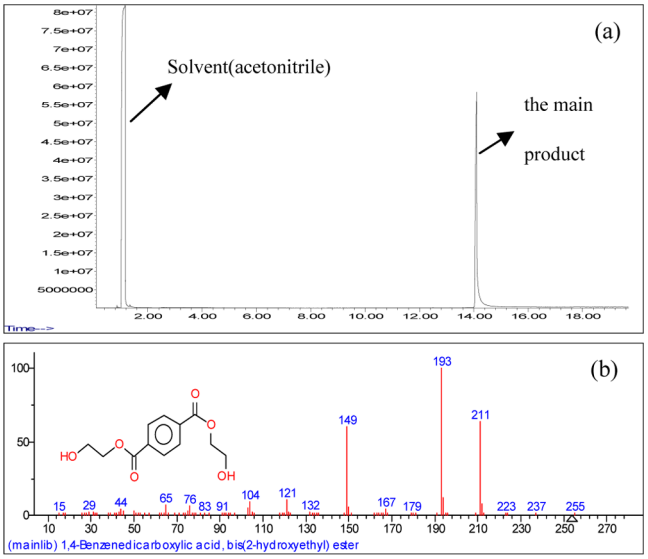

Figure 1. GC-MS spectra of the main product: (a) GC spectrum of the main product and (b) MS spectrum of the main product.

showed that the main product at 14.1 min in the GC chromatogram is BHET, and the product has high purity because there is no extra peak except the one for the solvent at 1.163 min (acetonitrile). ^{1}H NMR and ^{13}C NMR spectra are reproduced in Figure 2. The signal at δ 8.1 ppm indicates the presence of the four aromatic protons of the benzene ring. Signals at 4.3 and 3.7 ppm represent the methylene protons of COO−CH_2 and CH_2−OH, respectively. The peak at δ 4.9 ppm is characteristic of the protons of the hydroxyl. Moreover, the information on ^{13}C NMR is in accordance with those predicted in ^{1}H NMR, which also shown in Figure 2. It is clear from the ESI-MS in Figure 3 that the peak up to m/e 277 with intensity almost 100% was obtained. This peak is related to the main product ionized by Na^+ (in electrospray ionization, the fraction could be ionized by H^+, Na^+, or K^+). Thus, the molecular weight of the main product is 254 g/mol, which is the same as the molecular weight of BHET. At the same time, the only peak in the UPLC spectrum from Figure 4 indicates that purity of the main product obtained in our research is high. Element analysis results of the main product were compared with theoretical values of BHET in Table 2. It is clearly shown that the measured values of every elements in the main product are consistent with theoretical values of BHET and that the main product is chlorine free, which indicates that the main product is easily separated from the catalysts. Therefore, it can be

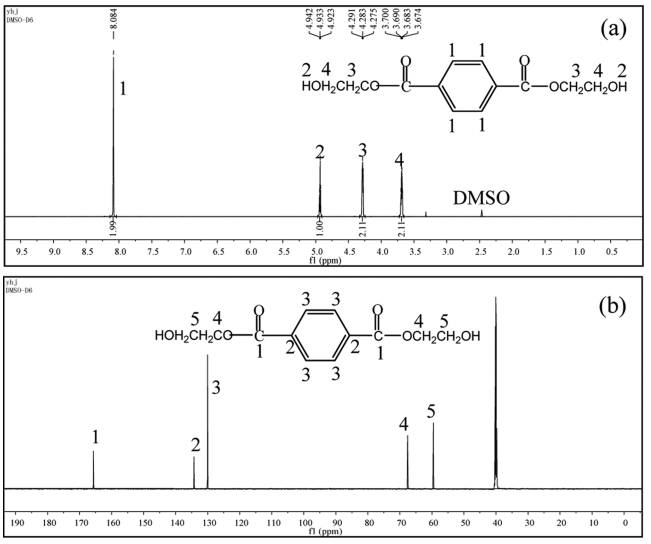

Figure 2. NMR patterns of the main product: (a) ^{1}HNMR patterns of the main product and (b) ^{13}CNMR patterns of the main product.

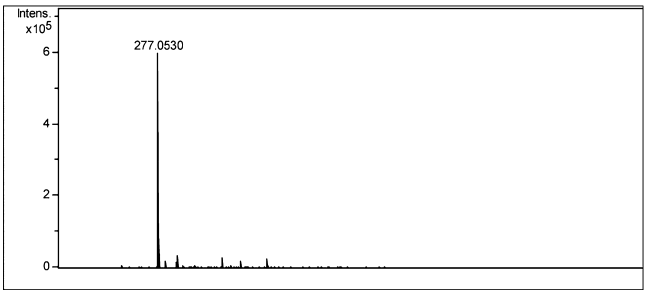

Figure 3. ESI-MS spectrum of the main product.

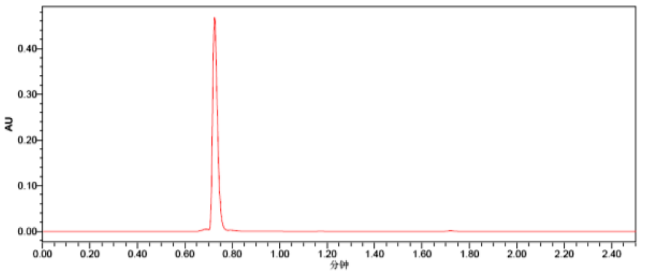

Figure 4. UPLC spectrum of the main product.

Table 2. Element Analysis Results of BHET

BHET	C (%)	H (%)	O (%)	Cl (%)
measured value	56.76	5.73	37.84	0
theoretical value	56.69	5.51	37.80	–

concluded from these characterizations that BHET with high purity can be effectively obtained by this method.

Physical properties of BHET were studied by XRD, SEM, DSC, and TGA. Figure 5 shows the XRD pattern of BHET in comparison with that of the PET material. PET exhibits a typical diffraction pattern due to the crystalline structure of this polyester, with broader diffraction peaks at 2θ = 16.4°, 17.7°, and 23.0°. Obviously, the diffraction peaks of BHET become narrower and are of higher relative intensity, which illustrates that BHET has high crystallinity and that its crystalline structure is different from that of PET. The diffraction angle,

DOI: 10.1021/sc5007522
ACS Sustainable Chem. Eng. 2015, 3, 340−348

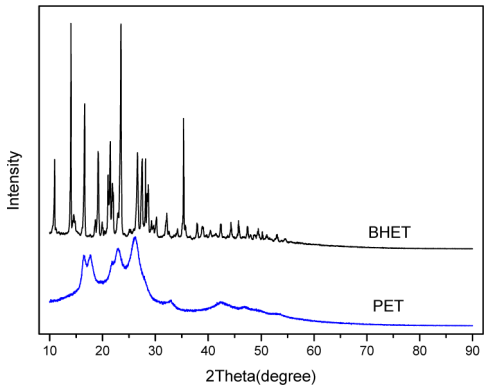

Figure 5. XRD patterns of PET and BHET.

crystal spacing, and relative intensity of BHET are shown in Table S2 of the Supporting Information. SEM images in Figure 6 clearly show that BHET has a columnar structure, which is

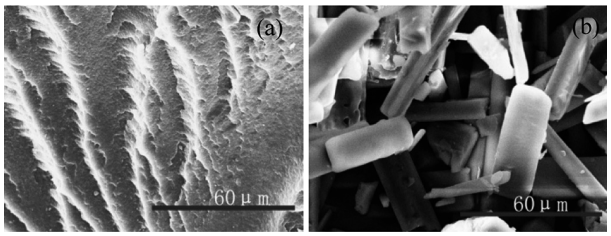

Figure 6. SEM images of PET material and the BHET: (a) SEM image of PET material and (b) SEM image of BHET.

different from that of the PET material. In the DSC curve in Figure 7, there is a sharp endothermic peak, and the melting

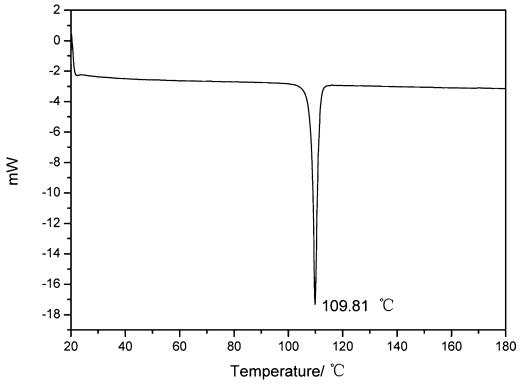

Figure 7. DSC curve of BHET.

onset temperature and peak temperature of BHET are 108.30 and 109.81 °C, respectively. The TGA curve of PET in Figure 8 shows significant weight loss at 410 °C. This weight loss is attributed to the thermal decomposition of the PET material. The TGA curve of BHET exhibits two clear weight loss processes. The first weight loss is about 32% with an onset temperature at 240 °C because of the thermal decomposition of BHET. The other weight loss is about 60% with an onset temperature at 409 °C because of the thermal decomposition of PET polymerized by BHET. These are both consistent with the literature.[11]

Influences of Reaction Conditions on PET Degradation. The synthesized first-row transition metal-containing ILs

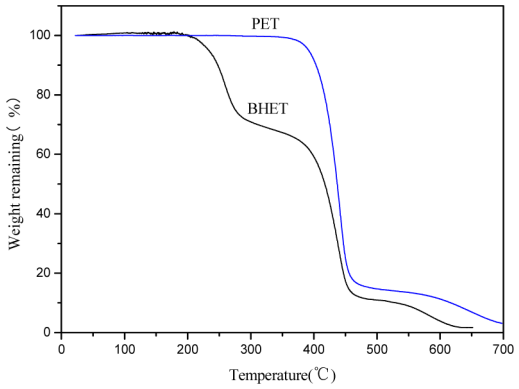

Figure 8. TGA curves of the PET material and BHET.

were used in the catalytic degradation of PET, and the results are summarized in Table 3. The results show that most of the

Table 3. Degradation of PET by Different IL Catalysts

source	cat.	conversion of PET (%)	selectivity of BHET (%)	mass fraction of BHET in products (wt %)
this work[a]	–	1.2	2.7	1.6
	$[bmim][CrCl_4]$[c]	1.7	4.2	2.3
	$[bmim][MnCl_3]$	86.7	72.1	84.7
	$[bmim][FeCl_4]$	94.7	58.9	76.4
	$[bmim]_2[CoCl_4]$	100	77.8	89.7
	$[bmim]_2[NiCl_4]$	45.0	64.3	74.7
	$[bmim]_2[CuCl_4]$	6.7	9.8	93.4
	$[bmim]_2[ZnCl_4]$	99.6	77.4	89.5
ref 9[b]	$[bmim][H_2PO_4]$[c]	6.9	–	–
	$[bmim][HSO_4]$[c]	0.5	–	–
	[bmim]Cl	44.7	–	–
	[bmim]Br	98.7	–	–

[a]Reacion conditions: PET size, 2.0 mm × 2.5 mm × 2.7 mm; PET, 5 g; EG, 20 g; cat., 1 g; 1 atm; 170 °C; and 4 h. [b]Reacion conditions: PET size, 2.0 mm × 2.5 mm × 2.7 mm; PET, 5 g; EG, 20 g; cat., 1 g; 1 atm; 180 °C; and 8 h. [c]Reaction temperature: dependent on the azeotropic temperatures of $[bmim][CrCl_4]$ and EG, 160 °C; $[bmim][H_2PO_4]$ and EG, 175 °C; and $[bmim][HSO_4]$ and EG, 170 °C.

first-row transition metal-containing ILs exhibit higher catalytic activity for degradation of PET than conventional ILs reported in the literature, such as [bmim]Cl, $[bmim][H_2PO_4]$, $[bmim][HSO_4]$, and [bmim]Br,[9] and $[bmim]_2[CoCl_4]$ and $[bmim]_2[ZnCl_4]$ show much higher depolymerization ability. However, PET did not dissolve in EG when $[bmim][CrCl_4]$ and $[bmim]_2[CuCl_4]$ were used as the catalysts. In the following study, we select $[bmim]_2[CoCl_4]$ as the catalyst.

The effect of PET particle size on degradation of PET is shown in Table 4. It shows that the time needed for complete degradation PET is gradually shortened with the decrease in PET particle size. When the PET particle size was 40−60 mesh, it only took 1.5 h for the complete degradation of PET, but the selectivity and mass fraction of BHET in products decreased slightly. This is because the smaller the particle size is, the more bumpy the particle surface and the greater the specific surface area that PET could interact with EG and catalyst; thus the complete degradation could be achieved in a shorter time. However, there is an equilibrium reaction between BHET and

DOI: 10.1021/sc5007522
ACS Sustainable Chem. Eng. 2015, 3, 340−348

Table 4. Influence of PET Particle Size on Degradation of PET[a]

PET particle size	time (h)	conversion of PET (%)	selectivity of BHET (%)	mass fraction of BHET in products (wt %)
2.0 mm × 2.5 mm × 2.7 mm	4	100	77.8	89.7
2.0 mm × 2.5 mm × 2.7 mm, ~12 mesh	3.5	100	74.2	89.3
12−14 mesh	3	100	74.1	89.0
14−20 mesh	2.2	100	73.8	88.7
20−30 mesh	1.8	100	73.5	88.6
40−60 mesh	1.5	100	73.4	88.3

[a]Reaction conditions: PET, 5 g; EG, 20 g; cat., 1 g; 1 atm; and 170 °C.

oligomers. The degraded BHET can polymerize into oligomers, resuting in decreased monomer selectivity.

Figure 9 presents the influence of the amount of the catalyst on the degradation of PET. It is observed that when the catalyst

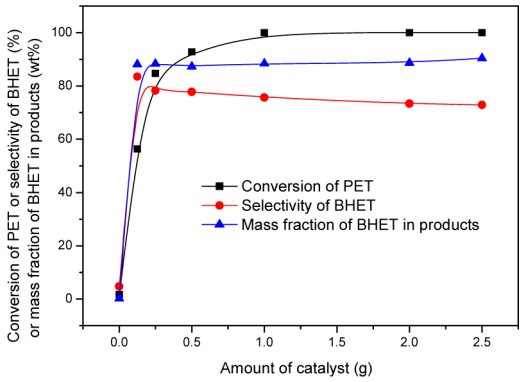

Figure 9. Effect of the amount of the catalyst on the degradation of PET. Reaction conditions: PET size, 40−60 mesh; PET, 5 g; EG, 20 g; 1 atm; 170 °C; and 1.5 h.

was added, the conversion of PET, selectivity of BHET, and mass fraction of BHET in products increased rapidly, much higher than the values obtained without catalyst. When the amount of catalyst was 1.0 g, the conversion of PET was 100%, and the mass fraction of BHET in products can reach more than 85% when the catalyst was added, a significant increase compared to 4.74% when no catalyst was added. Therefore, the catalyst significantly improves the glycolysis rate of PET. The selectivity of BHET first increases and then decreases slightly with an increase in the amount of catalyst. It may be that when a certain amount of catalyst was added, the initial degradation rate is faster, a large of monomer was accumulated rapidly in a short time, and part of the monomer was polymerized to dimers or oligomers in the heating process as the reaction further progresses.

The effect of reaction temperature on the degradation of PET is shown in Figure 10. It shows that the reaction temperature obviously influences the degradation of PET. The conversion of PET increases as the reaction temperature rises, which reaches 100% when the temperature is 175 °C or higher. The selectivity of BHET reaches a maximum value (77.8%) when the temperature is set at 170 °C with 92.8% PET conversion, and the variation trend of the mass fraction of BHET in the products is consistent with that of the selectivity of BHET, which may be that the high temperature is good for the PET chain being broken up into monomer units. However, higher temperature can make part of the BHET monomer polymerize into dimers or oligomers as the reaction progresses. In addition, the degradation of PET catalyzed by $[bmim]_2[CoCl_4]$ starts from 130 °C, lower than that catalyzed

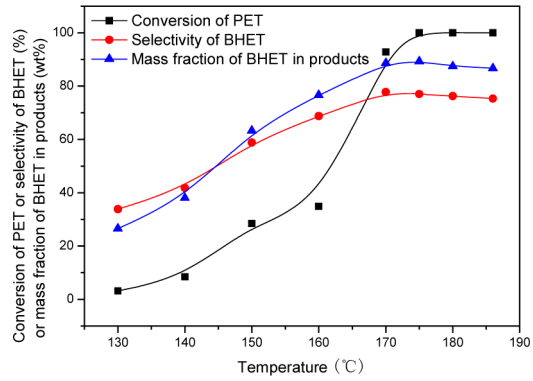

Figure 10. Effect of reaction temperature on the degradation of PET. Reaction conditions: PET size, 40−60 mesh; PET, 5 g; EG, 20 g; cat., 0.5 g; 1 atm; and 1.5 h.

by $[bmim][FeCl_4]$ (140 °C) and traditional catalysts, such as zinc acetate (150 °C).[26,30] Therefore, $[bmim]_2[CoCl_4]$ has the best low-temperature catalytic activity for the degradation of PET in EG, and this catalytic glycolysis process is more energy efficient.

Figure 11 presents the influence of reaction time on the degradation of PET. It is observed that with an increase in

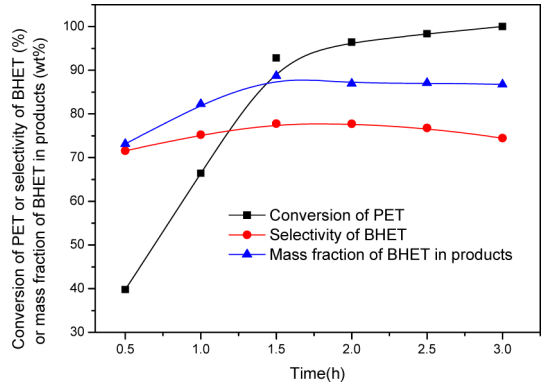

Figure 11. Effect of reaction time on the degradation of PET. Reaction conditions: PET size, 40−60 mesh; PET, 5 g; EG, 20 g; cat., 0.5 g; 1 atm; and 170 °C.

reaction time from 0.5 to 3.0 h, the conversion of PET increases sharply. When the reaction time was extended to 3 h, the conversion of PET could reach 100% at a reaction temperature of 170 °C. The selectivity and mass fraction of BHET in products reach maximum values (77.8% and 88.7%) when the reaction time was 1.5 h. This is because there is an equilibrium reaction between BHET and oligomers. With the reaction time extending, the BHET will polymerize into oligomers.

DOI: 10.1021/sc5007522
ACS Sustainable Chem. Eng. 2015, 3, 340−348

Figure 12 presents the influence of the amount of EG on the degradation of PET. It shows that PET conversion stays at

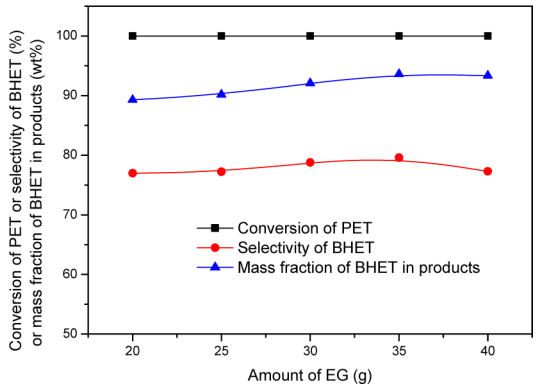

Figure 12. Effect of the amount of EG on the degradation of PET. Reaction conditions: PET size, 40−60 mesh; PET, 5 g; cat., 0.5 g; 1 atm; 175 °C; and 1.5 h.

100% with an increase in the amount of EG from 20 to 40 g, while BHET selectivity and mass fraction of BHET in products both have maximum values at 35 g. The maximum values are 79.6% and 93.6%, respectively. This may be attributed to the concentration change of the catalyst, which will affect the contact area among catalyst, EG, and PET.

Figure 13 presents the influence of the amount of PET on the degradation of PET. It shows that PET can be competely

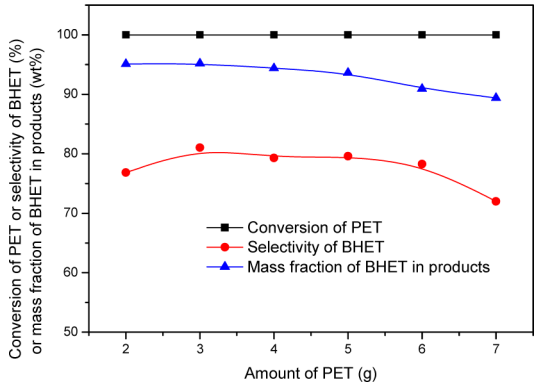

Figure 13. Effect of the amount of PET on the degradation of PET. Reaction conditions: PET size, 40−60 mesh; cat., 0.5 g; 1 atm; 175 °C; and 1.5 h.

degraded with an increase in the amount of PET from 2 to 7 g, while the selectivity and mass fraction of BHET in products have maximum values (81.1% and 95.7%, respectively) when the amount of PET is 3 g because the mass ratio of PET, EG, and catalyst can infulence the equilibrium shift between BHET and oligomers.

PET particle size, reaction temperature, and reaction time play key roles in the degradation of PET, and the optimization conditions were obtained by the study on the effects of reaction conditions. Under the optimization conditions (EG, 35 g; $[bmim]_2[CoCl_4]$, 0.5 g; PET, 3 g; PET size, 40−60 mesh; 175 °C; and 1.5 h), the conversion of PET, selectivity of BHET, and mass fraction of BHET in products are 100%, 81.1%, and 95.7%, respectively.

Recycling of Residual EG and Catalyst. From the viewpoint of environmental conservation and the economics of the process, recycling of the residual EG and the catalyst is absolutely required after the degradation of PET. After BHET was filtered from the liquid phase, the residual EG and catalyst in the filtrate were recovered by vacuum evaporation at 65 °C, stored in a vacuum oven at 60 °C for 12 h, and then supplied a certain amount of EG until the weight is equal to the initial weight of fresh EG and catalyst. The conversion of PET in recycled EG and $[bmim]_2[CoCl_4]$ was detected, and the result is listed in Table 5. It shows that recycled $[bmim]_2[CoCl_4]$ still kept high catalytic activity and worked efficiently in the sixth recycling.

Table 5. Recycling and Reuse of Residual EG and $[bmim]_2[CoCl_4]$[a]

recycle times	conversion of PET (%)	selectivity of BHET (%)	mass fraction of BHET in products (wt %)
0	100	81.1	95.7
1	100	83.9	97.1
2	100	83.2	96.8
3	100	81.8	95.9
4	100	82.5	95.4
5	100	81.7	95.6
6	100	81.0	95.1

[a]Reaction conditions: PET size, 40−60 mesh; PET, 3 g; EG, 35 g; cat., 0.5 g; 1 atm; 175 °C; and 1.5 h.

The recovered $[bmim]_2[CoCl_4]$ after recycling six times was characterized by FT-IR and Raman spectra in comparison with the fresh one. The results are shown in Figures 14 and 15. It is

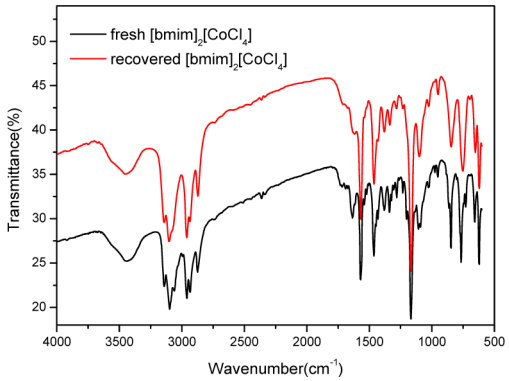

Figure 14. IR spectra of fresh $[bmim]_2[CoCl_4]$ and recovered $[bmim]_2[CoCl_4]$.

shown in Figure 14 that the characteristic peaks in the IR spectrum of the recovered $[bmim]_2[CoCl_4]$ are consistent with that of the fresh one, and the Raman spectra in Figure 15 show the same results, which explain that the structure of the recovered catalyst after recycling six times has not been changed.

Degradation Mechanism of PET. The reaction process showed a beautiful color change. It changed gradually from pink to blue with the temperature increasing from 20 to 120 °C and then kept blue from 120 °C to the reaction temperature. The color comes back to pink from blue when the temperature decreased from reaction temperature to 120 °C and kept pink from 120 to 20 °C. This maybe results from the interaction between EG and the catalyst.[32] In-situ IR spectra of the reactants are given in Figure 16. It is shown that the hydroxyl vibration shows an obvious 70 cm^{-1} red shift from 3376 to

DOI: 10.1021/sc5007522
ACS Sustainable Chem. Eng. 2015, 3, 340−348

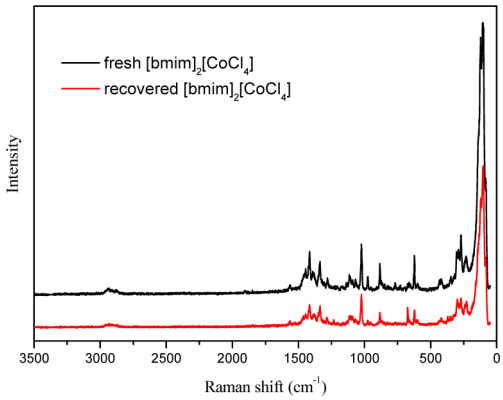

Figure 15. Raman spectra of fresh $[bmim]_2[CoCl_4]$ and recovered $[bmim]_2[CoCl_4]$.

3448 cm^{-1} with the temperature increasing from 20 to 170 °C using $[bmim]_2[CoCl_4]$ as the catalyst, as shown in Figure 16(a). But the red shift of the hydroxyl vibration is only 34 cm^{-1} when the reactant is only EG, shown in Figure 16(b). This indicates that the interaction between EG and catalyst can activate the hydroxy in EG and then enhance its ability to interact with the ester group in PET. To further understand the effect of the interaction between EG and catalysts on the PET degradation, the in situ IR spectra using $[bmim][CrCl_4]$ and $[bmim][FeCl_4]$ as the catalysts were also measured. The red shifts of the hydroxyl vibration also happened and are 37 and 42 cm^{-1}, respectively. So the intensity of the red shifts follows the order: $[bmim]_2[CoCl_4]$ > $[bmim][FeCl_4]$ > $[bmim][CrCl_4]$ > without catalyst. The order is consistent with the catalytic activity of these catalysts in the glycolysis process of PET, which further explains that the interaction between EG and catalyst can promote PET glycolysis and plays an important role in the PET glycolysis process.

Therefore, a mechanism of PET degradation catalyzed by $[bmim]_2[CoCl_4]$ is proposed based on the in situ IR and experimental results and is illustrated in Scheme 1. $[CoCl_4]^{2-}$ first interacts with the hydrogen of the hydroxyl in EG and $[bmim]^+$ interacts with the oxygen in the ester of PET. Then the oxygen in the ester of PET attacks the carbon cation of the ester group in PET more easily and finally results in the disconnection of the long molecule chain of PET. The higher catalytic activity might be attributed to the synergic effect between cation and anion of the catalysts.

CONCLUSIONS

First-row transition metal-containing ILs have good thermal stability and can catalyze the degradation of PET in EG. $[Bmim]_2[CoCl_4]$ and $[bmim]_2[ZnCl_4]$ exhibit higher catalytic activity under mild reaction conditions. The influences of experimental parameters on the degradation of PET were investigated when $[bmim]_2[CoCl_4]$ was used as the catalyst. PET particle size, reaction temperature, and reaction time play key roles in the degradation of PET. The recycled experiments show that $[bmim]_2[CoCl_4]$ worked efficiently, although it had been used six times, which overcame the drawback that conventional catalysts are difficult to recycle. Moreover, based on in situ IR spectra and experimental phenomenon, the mechanism of this degradation process was proposed and showed that the high catalytic activity was attributed to $[CoCl_4]^{2-}$ interacting with the hydrogen of the hydroxyl in EG and the $[bmim]^+$ interacting with the oxygen in the ester of

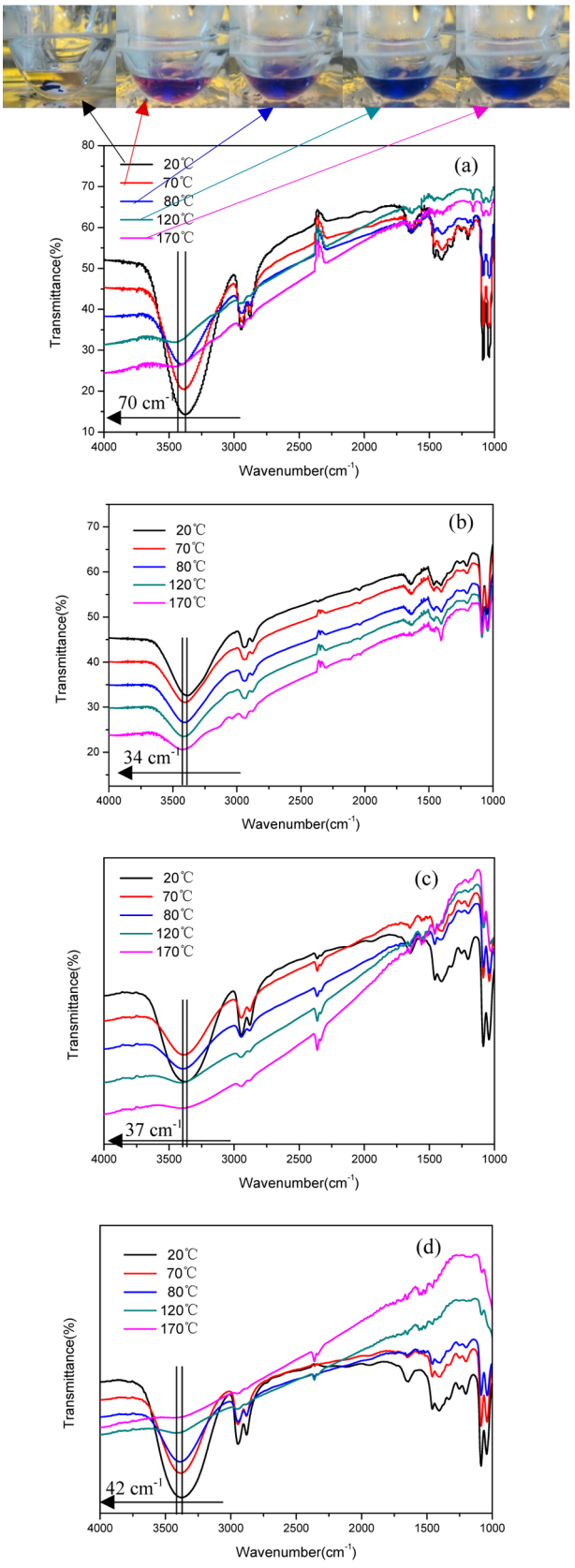

Figure 16. In-situ IR spectra: (a) The color changes during reaction process and in situ IR spectra of reactants catalyzed by $[bmim]_2[CoCl_4]$. (b) In situ IR spectra of EG. (c) In situ IR spectra of EG catalyzed by $[bmim][CrCl_4]$. (d) In situ IR spectra of EG catalyzed by $[bmim][FeCl_4]$.

DOI: 10.1021/sc5007522
ACS Sustainable Chem. Eng. 2015, 3, 340−348

Scheme 1. Proposed Mechanism for Degradation of PET

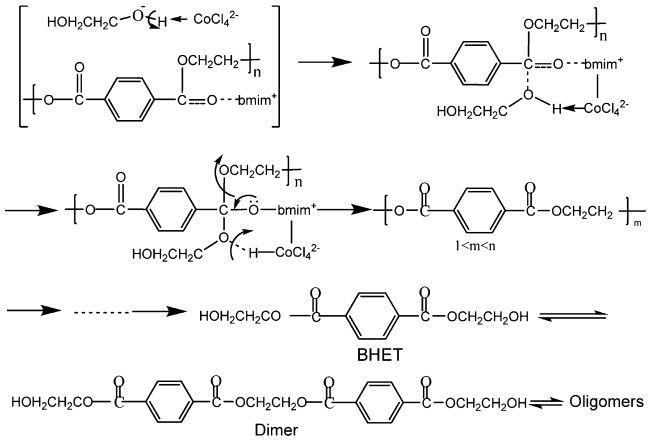

PET. It is believed that this study provides much important information for the efficient recycling of PET wastes, and those ILs with metal complex anions can be used for many purposes, not just catalysts, due to their good thermal stability and magnetic, catalytic, and optical properties.

■ ASSOCIATED CONTENT

Supporting Information

TGA curves of [bmim]Cl and $[bmim]_2[CoCl_4]$, element analysis results of [bmim]Cl/$CoCl_2$, and XRD results of BHET. This material is available free of charge via the Internet at http://pubs.acs.org.

■ AUTHOR INFORMATION

Corresponding Authors

*Tel/Fax: (+86)-10-8262-7080. E-mail: xmlu@ipe.ac.cn (X.L.). Web site: http://ilct.mpcs.cn.

*Tel/Fax: (+86)-10-8262-7080. E-mail: sjzhang@ipe.ac.cn (S.Z.). Web site: http://ilct.mpcs.cn.

Notes

The authors declare no competing financial interest.

■ ACKNOWLEDGMENTS

This work was supported financially by the Program of National High Technology Research and Development Program of China (2012AA063001), National Natural Science Foundation of China (21276255), Shandong Province Natural Science Foundation (ZR2014BQ018), and Beijing Natural Science Foundation of China (2131005 and 2132055).

■ REFERENCES

(1) Rostami, A.; Wei, C. J.; Guerin, G.; Taylor, M. S. Anion detection by a fluorescent poly(squaramide): Self-assembly of anion-binding sites by polymer aggregation. *Angew. Chem., Int. Ed.* **2011**, *50*, 2059–2062.

(2) Huck, W. T. S. Materials chemistry polymer networks take a bow. *Nature* **2011**, *472*, 425–426.

(3) Xi, G. X.; Lu, M. X.; Sun, C. Study on depolymerization of waste polyethylene terephthalate into monomer of bis(2-hydroxyethyl terephthalate). *Polym. Degrad. Stab.* **2005**, *87*, 117–120.

(4) Ghaemy, M.; Mossaddegh, K. Depolymerisation of poly(ethylene terephthalate) fibre wastes using ethylene glycol. *Polym. Degrad. Stab.* **2005**, *90*, 570–576.

(5) Bartolome, L.; Imran, M.; Lee, K. G. Superparamagnetic γ-Fe_2O_3 nanoparticles as an easily recoverable catalyst for the chemical recycling of PET. *Green Chem.* **2014**, *16*, 279–286.

(6) El Mejjatti, A.; Harit, T.; Riahi, A.; Khiari, R.; Bouabdallah, I.; Malek, F. Chemical recycling of poly(ethylene terephthalate). Application to the synthesis of multiblock copolyesters. *Express Polym. Lett.* **2014**, *8*, 544–553.

(7) Kueh, H. Y.; Mitchison, T. J. Structural plasticity in actin and tubulin polymer dynamics. *Science* **2009**, *325*, 960–963.

(8) Liu, F. S.; Cui, X.; Yu, S. T.; Li, Z.; Ge, X. P. Hydrolysis reaction of poly(ethylene terephthalate) using ionic liquids as solvent and catalyst. *J. Appl. Polym. Sci.* **2009**, *114*, 3561–3565.

(9) Wang, H.; Liu, Y. Q.; Li, Z. X.; Zhang, X. P.; Zhang, S. J.; Zhang, Y. Q. Glycolysis of poly(ethylene terephthalate) catalyzed by ionic liquids. *Eur. Polym. J.* **2009**, *45*, 1535–1544.

(10) Baliga, S.; Wong, W. T. Depolymerization of poly(ethylene terephthalate) recycled from post-consumer soft-drink bottles. *J. Polym. Sci., Polym. Chem.* **1989**, *27*, 2071–2082.

(11) Chen, C. H. Study of glycolysis of poly(ethylene terephthalate) recycled from postconsumer soft-drink bottles. III. Further investigation. *J. Appl. Polym. Sci.* **2003**, *87*, 2004–2010.

(12) Troev, K.; Grancharov, G.; Tsevi, R.; Gitsov, I. A. novel catalyst for the glycolysis of poly(ethylene terephthalate). *J. Appl. Polym. Sci.* **2003**, *90*, 1148–1152.

(13) Lee, H. N.; Lodge, T. P. Poly(n-butyl methacrylate) in ionic liquids with tunable lower critical solution temperatures (LCST). *J. Phys. Chem. B* **2011**, *115*, 1971–1977.

(14) Torrecilla, J. S.; Rodriguez, F.; Bravo, J. L.; Rothenberg, G.; Seddond, K. R.; Lopez-Martin, I. Optimising an artificial neural network for predicting the melting point of ionic liquids. *Phys. Chem. Chem. Phys.* **2008**, *10*, 5826–5831.

(15) Hough, W. L.; Smiglak, M.; Rodriguez, H.; Swatloski, R. P.; Spear, S. K.; Daly, D. T.; Pernak, J.; Grisel, J. E.; Carliss, R. D.; Soutullo, M. D.; Davis, J. H.; Rogers, R. D. The third evolution of ionic liquids: Active pharmaceutical ingredients. *New J. Chem.* **2007**, *31*, 1429–1436.

(16) Armand, M.; Endres, F.; MacFarlane, D. R.; Ohno, H.; Scrosati, B. Ionic-liquid materials for the electrochemical challenges of the future. *Nat. Mater.* **2009**, *8*, 621–629.

(17) Cooper, E. R.; Andrews, C. D.; Wheatley, P. S.; Webb, P. B.; Wormald, P.; Morris, R. E. Ionic liquids and eutectic mixtures as solvent and template in synthesis of zeolite analogues. *Nature* **2004**, *430*, 1012–1016.

(18) Rogers, R. D.; Seddon, K. R. Ionic liquids—Solvents of the future? *Science* **2003**, *302*, 792–793.

(19) Wang, H.; Li, Z. X.; Liu, Y. Q.; Zhang, X. P.; Zhang, S. J. Degradation of poly(ethylene terephthalate) using ionic liquids. *Green Chem.* **2009**, *11*, 1568–1575.

(20) Wang, H.; Gurau, G.; Rogers, R. D. Ionic liquid processing of cellulose. *Chem. Soc. Rev.* **2012**, *41*, 1519–1537.

(21) Chiappe, C.; Pomelli, C. S.; Bardi, U.; Caporali, S. Interface properties of ionic liquids containing metal ions: features and potentialities. *Phys. Chem. Chem. Phys.* **2012**, *14*, 5045–5051.

(22) Wang, H.; Yan, R. Y.; Li, Z. X.; Zhang, X. P.; Zhang, S. J. Fe-containing magnetic ionic liquid as an effective catalyst for the glycolysis of poly(ethylene terephthalate). *Catal. Commun.* **2010**, *11*, 763–767.

(23) Zhou, X. Y.; Lu, X. M.; Wang, Q.; Zhu, M. L.; Li, Z. X. Effective catalysis of poly(ethylene terephthalate) (PET) degradation by metallic acetate ionic liquids. *Pure Appl. Chem.* **2012**, *84*, 789–801.

(24) Lin, I. J. B.; Vasam, C. S. Metal-containing ionic liquids and ionic liquid crystals based on imidazolium moiety. *J. Organomet. Chem.* **2005**, *690*, 3498–3512.

(25) Sitze, M. S.; Schreiter, E. R.; Patterson, E. V.; Freeman, R. G. Ionic liquids based on $FeCl_3$ and $FeCl_2$. Raman scattering and ab initio calculations. *Inorg. Chem.* **2001**, *40*, 2298–2304.

(26) Kozlova, S. A.; Verevkin, S. P.; Heintz, A.; Peppel, T.; Kockerling, M. Paramagnetic ionic liquid 1-butyl-3-methylimidazolium tetrabromidocobaltate(II): Activity coefficients at infinite dilution of organic solutes and crystal structure. *J. Chem. Eng. Data* **2009**, *54*, 1524–1528.

DOI: 10.1021/sc5007522
ACS Sustainable Chem. Eng. 2015, 3, 340–348

(27) Zhang, P. F.; Gong, Y. T.; Lv, Y. Q.; Guo, Y.; Wang, Y.; Wang, C. M.; Li, H. R. Ionic liquids with metal chelate anions. *Chem. Commun.* **2012**, *48*, 2334−2336.
(28) Welton, T. Ionic liquids in catalysis. *Coord. Chem. Rev.* **2004**, *248*, 2459−2477.
(29) Hallett, J. P.; Welton, T. Room-temperature ionic liquids: Solvents for synthesis and catalysis. 2. *Chem. Rev.* **2011**, *111*, 3508−3576.
(30) Chen, C. H.; Chen, C. Y.; Lo, Y. W.; Mao, C. F.; Liao, W. T. Studies of glycolysis of poly(ethylene terephthalate) recycled from postconsumer soft-drink bottles. I. Influences of glycolysis conditions. *J. Appl. Polym. Sci.* **2001**, *80*, 943−948.
(31) Goje, A. S.; Mishra, S. Chemical kinetics, simulation, and thermodynamics of glycolytic depolymerization of poly(ethylene terephthalate) waste with catalyst optimization for recycling of value added monomeric products. *Macromol. Mater. Eng.* **2003**, *288*, 326−336.
(32) Bi, W. Z. The thermochromism of $CoCl_2$ in the mixture of EtOH and H_2O. *J. Suzhou Univ.* **1990**, *4*, 515−519.

DOI: 10.1021/sc5007522
ACS Sustainable Chem. Eng. 2015, 3, 340−348